



Sizing of delamination using time-of-flight of the fundamental symmetric Lamb modes

C. Ramadas¹, Avinash Hood¹, Janardhan Padiyar²,
 Krishnan Balasubramaniam² and Makarand Joshi¹

Abstract

In this study, a procedure is devised, using the fundamental symmetric Lamb mode (S_0) to estimate the size of an impact-induced delamination at the bottom interface of a composite laminate, which has been subjected to a low-velocity impact. When S_0 mode incidents at the edge of delamination, it propagates independently in 0° layer and the rest of layers. Based on the propagation of S_0 mode in the delaminated region, an expression is derived, which can estimate the size of interface delamination using measured arrival times or Time-of-Flight (ToF) of S_0 modes. Numerical simulations were carried out on glass/epoxy (GFRP) cross-ply laminates ($[0/90_2]_s$) to confirm the derived expression and eventually it was validated through experiments carried out on $[0/90/0]$ GFRP laminates. Moreover, the minimum detectable size of delamination through the proposed method was estimated analytically and verified through numerical simulations.

Keywords

Lamb wave, delamination, impact, time-of-flight, finite element analysis

Introduction

The superiority of composite materials compared to metals is due to their high specific strength and specific modulus. The other added advantages of composite materials are excellent fatigue-performance and corrosion-free maintenance. Because of this, composites are extensively used in military and aerospace industries for load-bearing applications.

In general, the damages that composites encounter are more severe than their metallic counterparts are prone to. Delamination is one such damage, which debilitates the structure in compression and bending loads. This damage is sub-surface in nature. It cannot be gauged by the naked eye. Delamination-type damage usually occurs on account of low-velocity impact caused in turn by bird hits, debris on the runway or even something as simple as the dropping of a tool, during maintenance. For safe operation of composite structures, quick and frequent inspection techniques are required. Conventional C-scan and X-ray techniques are tedious and time-consuming. There is an urgent need for the development of new inspection/

non-destructive evaluation techniques for composite structures.

Lamb waves are ultrasonic waves which propagate in thin structural waveguides, whose thickness is much less than the wave length of the Lamb modes.¹ When a Lamb mode propagates in a thin plate, all the particles across the thickness of plate undergo in-plane and out-of-plane deformations. Due to this, when a Lamb mode encounters a sub-surface damage, it gets modulated and gives rise to mode conversion, change in velocity, reduction in amplitude, scattering, reflection, etc. In general, all these features are explored in Lamb wave-based damage detection techniques.

¹Composite Research Center, R & D E (E), Dighi, India.

²Center for Non-Destructive Evaluation, Department of Mechanical Engineering, Indian Institute of Technology Madras, India.

Corresponding author:

Krishnan Balasubramaniam, Center for Non-Destructive Evaluation, Department of Mechanical Engineering, Indian Institute of Technology Madras, Chennai-600 036, India
 Email: balas@iitm.ac.in

Earlier, studies were carried out on interaction of S_0 Lamb mode with delaminations in cross-ply laminates.² Wave groups reflected from the delamination edges were studied. When a delamination was located symmetrically across the thickness of the plate, no reflections were observed. This was attributed to zero shear stress at the delamination interface. The reflected wave groups were used to locate the delamination.³ When a Lamb wave propagates through a defect, wave velocity reduces due to reduction in local stiffness. Some work was carried out to detect damage in composites based on this phenomenon.⁴⁻⁸

Valdes and Soutis⁹ and Ip and Mai¹⁰ detected delaminations in composite laminates using the reflected wave groups from delamination edge. Su and Ye¹¹ developed a Lamb wave-based quantitative technique, using artificial neural network, for identifying delaminations in CF/EP composite structures. Dufflo et al.¹² characterized defects in the bonding of carbon/epoxy (CFRP) composite laminates using Lamb waves. Air-coupled transducers were used to obtain C-scan images of the transmitted signal when the plate was moving between the two transducers. Contact transducer and laser interferometer were used for studying Lamb wave propagation through the defect. The size and flaw area were estimated. Toyama and Takatsubo¹³ proposed an inspection technique using symmetric Lamb mode (S_0) to detect impact-induced delamination in composite laminates. This technique requires two line scans. Change in wave velocity and amplitude, due to delamination, were the criteria used for damage detection.

Hayashi and Kawashima¹⁴ studied the reflection of Lamb modes at the delamination edges through strip element^{15,16} based numerical models. Palacz et al.¹⁷ studied the propagation of flexural-shear coupled wave in a delaminated multi-layered composite beam, using spectral finite element (FE) method. Ramadas et al.¹⁸⁻²⁰ studied through numerical simulations and experiments, the interaction of A_0 mode with symmetric and asymmetric delaminations in composite plates. Based on these studies, a methodology was proposed to detect the size of delamination using A_0 and mode converted A_0 modes. This technique does not require a signal from healthy region.²⁰

In this study, a methodology to detect the delamination size due to low-velocity impact is worked out using ToF of S_0 modes propagating in the delaminated region. An expression was derived based on the propagation of S_0 mode through the sub-laminates, which were formed due to delamination at that location. Initially, this expression was verified on $[0/90_2]_s$ cross-ply laminate through numerical simulations and eventually experimental verification was carried out on $[0/90/0]$ cross-ply laminate. The minimum detectable delamination size is also estimated through a supplementary equation.

S_0 mode propagation through delamination

In low-frequency thickness region, the velocity of S_0 mode is higher than that of A_0 mode. The influence of in-plane stiffness on S_0 mode velocity is higher than that on A_0 mode velocity. It was demonstrated that in cross-ply laminates ($[0/90_n]_s$), due to delamination no interfacial continuity between layers 0° and 90° exists.^{4,5} Because of this, Lamb mode propagates independently in these layers. In impact type damage, multiple delaminations start at various interfaces in cross-ply and quasi-isotropic laminates. From analytical and experimental studies,²¹⁻²⁵ it was concluded that in low-velocity impact damage, the delamination starts at the bottom-most ply and propagates in the direction of fibers for both the cross-ply and quasi-isotropic laminates. The delaminated area resulting from low-velocity impact has an oblong shape ('peanut shape') inclined toward the direction of fibers, in the lower plies at the interface.²⁶ When S_0 mode propagates in the delaminated region, the wave propagates independently in 0° layer and rest of the layers.¹³ Since S_0 mode velocity depends on in-plane stiffness, its velocity is high in 0° layer (thin sub-laminate) than that in rest of the laminate (thick sub-laminate). Based on the above discussion, Toyama and Takatsubo¹³ derived the following expression:

$$t_i - t_o = L \left(\frac{1}{V_i} - \frac{1}{V_o} \right) \quad (1)$$

where V_i and V_o are S_0 mode velocities of the healthy laminate and 0° layers, respectively, and t_i and t_o are the corresponding arrival times. Equation (1) can be used to evaluate quantitatively the length of delamination at bottom interface (L), due to low-velocity impact, by measuring the arrival time of transmitted wave group along 0° direction. Toyama and Takatsubo¹³ demonstrated experimentally, the procedure to evaluate the delamination type damage. In Equation (1), to estimate the delamination size, a reference signal from healthy region is required. While deriving Equation (1), there is an explicit assumption that the distance between the transmitter and receiver should not change while capturing the signals at healthy and delaminated regions.

It was shown in the study of Toyama and Takatsubo¹³ that S_0 mode propagates in 0° layer and the rest of the laminate independently. The main characteristic of low-velocity impact-induced delamination is that the size of delamination at the bottom-most interface is higher than that at other interfaces. In cross-ply laminates ($[0/90_n]_s$ and $[0/90]_{ns}$) 0° layers are always positioned at the top and bottom surfaces, followed by 90° layers. In impact-induced delamination,

the size of interface delamination at the bottom 0° and 90° layers is maximum. Above this 90° layer, there may be either 90° or 0° layer. The size of delamination between these two layers will be less than that at the bottom most interface. As we move ahead towards the top most layers, the sizes of delamination between interfaces will gradually reduce and some interfaces may not have any delamination. For instance, assume that S_o is generated at the transmitter, as shown in Figure 1. S_o mode propagates in the main laminate and incidents at the front edge of delamination (P). It splits here and propagates independently in bottom 0° layer and the other layers. The top interfaces may not have any delaminations. Even if they have, the sizes of delaminations are much smaller than at the bottom most. S_o modes propagating in the top layers have lower velocity (because of majority of 90° layers) than in the bottom 0° layer, and also S_o modes undergo interferences at the exit of delamination and propagate as a single S_o mode in the main laminate. From this analysis, it is inferred that S_o modes propagate independently in 0° layer and the rest of the laminate in an impact-induced delaminated region. Since the in-plane stiffness of 0° layer is greater than that of the rest, S_o mode propagates faster in 0° layer. The S_o mode in 0° layer reaches the rear edge of delamination (Q) faster than its counterpart propagating in the rest. Based on the size of delamination, the wave groups on reaching Q either undergo interference or propagate independently in the main laminate. Based on this propagation phenomenon, the following equation can be derived:

$$\Delta t = t_2 - t_1 = L \left(\frac{1}{V_1} - \frac{1}{V_2} \right) \quad (2)$$

where t_1 and t_2 are the arrival times of S_o mode in 0° layer and rest of the layers, respectively. Since S_o mode has higher velocity than A_o , the first two wave groups at the leading edge of the captured signal correspond

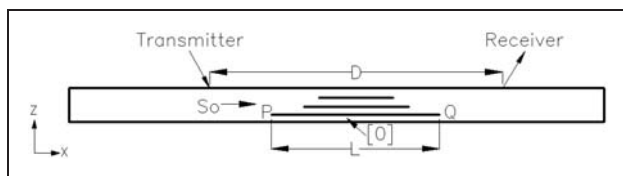


Figure 1. Propagation of S_o mode in a delaminated composite laminate.

those propagated through 0° layer and rest of the layers. Equation (2) was validated through numerical modeling and eventually through experimentation.

Numerical modeling

All numerical simulations were carried out using FE code ANSYS²⁷ on glass/epoxy (GFRP) cross-ply laminate having lay-up $[0/90_2]_s$. Numerical simulations were carried out on four different sizes of delaminations, 70, 65, 60, 55, and 45 mm. In the following paragraphs, the procedure adopted for numerical modeling on $[0/90_2]_s$ laminate, containing 60-mm size delamination is described in detail.

In the given laminate, there were six plies (two 0° plies and four 90° plies). In FE model, each ply was modeled separately and the properties were attributed. The thickness and length of each ply were 0.33 and 300 mm, respectively. The total thickness of laminate worked out to 1.98 mm. The properties of glass/epoxy lamina are shown in Table 1. The central frequency of excitation and number of cycles were 200 kHz and 5, respectively. The excitation pulse was a tone burst modulated with Hanning window. The element used for modeling was an eight-node plane strain element with two translational degrees of freedom at each node. The size of element was 0.165 mm in the thickness direction and 0.25 mm in length direction. Attenuation was not considered in numerical modeling. Delamination was modeled by de-merging the nodes at the delamination region.² To excite pure

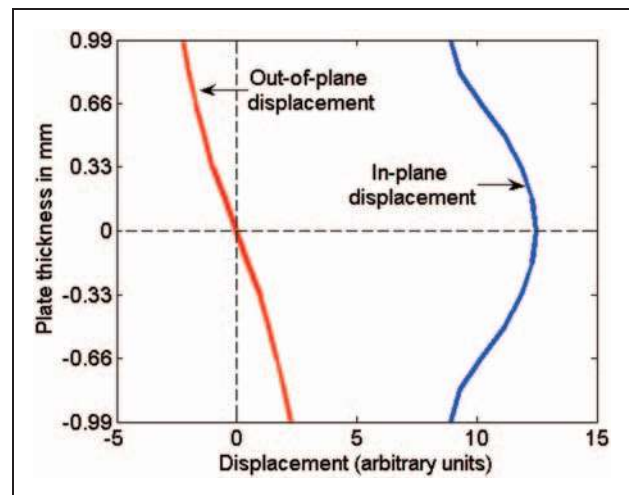


Figure 2. In-plane and out-of-plane displacement patterns to be given across plate thickness to excite S_o mode at 200 kHz.

Table 1. Material properties

Material	E_{11} (GPa)	E_{22} (GPa)	ν_{13}	ν_{23}	G_{13} (GPa)	ρ (kg/m^3)
Glass/epoxy	44.68	6.90	0.280	0.355	2.54	1990

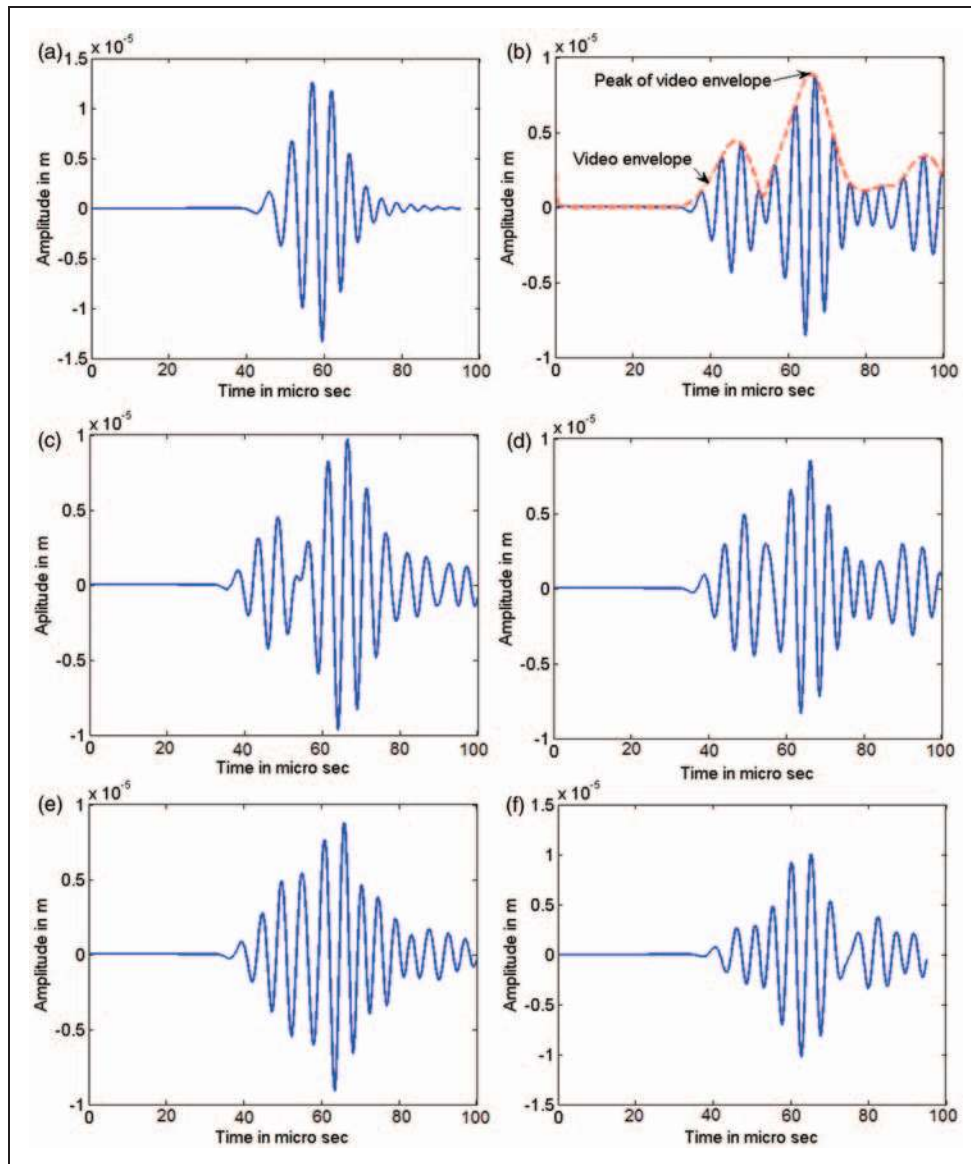


Figure 3. A-scans from numerical simulations captured at (a) 0 mm, (b) 70 mm, (c) 65 mm, (d) 60 mm, (e) 55 mm, and (f) 45 mm delamination locations.

S_0 mode in $[0/90_2]_s$ laminate at 200 kHz, the in-plane and out-of-plane displacement patterns (obtained from DISPERSE²⁸) to be given to the particles across the thickness of plate are shown in Figure 2. S_0 mode in the main laminate was excited by giving this displacement pattern across the thickness of plate. Similar procedure was adopted to model the other delamination sizes as well. The group velocities of S_0 mode in 0° layer and the rest, obtained from DISPERSE, are 4765.9 m/s and 2064.1 m/s, respectively.

The distance of separation between the transmitter and receiver was 120 mm (D), as shown in Figure 1. Initially, numerical simulation was carried out in the intact/healthy region. A-scan obtained at healthy region is shown in Figure 3(a). Since there was no delamination

in the path of propagation, S_0 mode did not get modulated. A-scans obtained at 70, 65, 60, 55, and 45 mm regions are shown in Figure 3(b)–(f), respectively. A video envelope was fitted over each A-scan. The peak of this envelope, shown in Figure 3(b), was taken as the representative arrival time of that whole wave group. The size of delamination was estimated using Equation (2). Table 2 lists the estimated delamination sizes in all four cases.

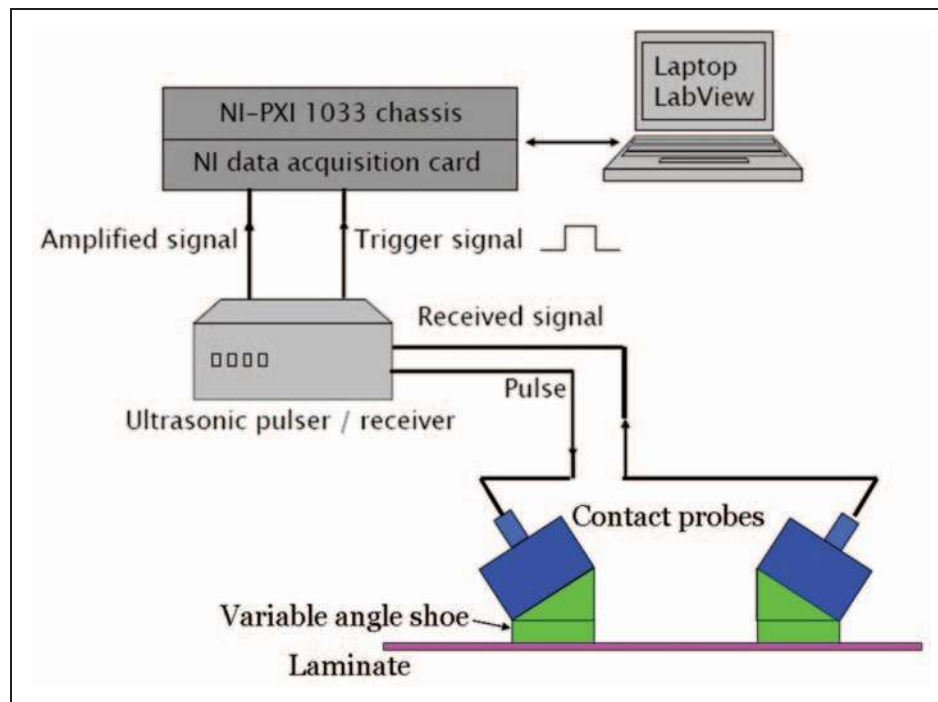
Experimental work

Fabrication of specimen

Experiments were carried out on cross-ply laminates. Two glass/epoxy laminates of $[0/90/0]$ lay-up, with

Table 2. Predicted delamination sizes from arrival times of S_0 modes in numerical modeling on $[0/90_2]_s$ laminate

Actual delamination size (mm)	t_1 (μs)	t_2 (μs)	$\Delta t = t_2 - t_1$ (μs)	Predicted delamination size, L (mm)
70	46.4	65.95	19.55	71.1
65	47.85	65.4	17.55	63.9
60	49.5	65.3	15.8	57.5
55	49.7	64.35	14.65	53.3

**Figure 4.** Schematic of experimental setup.

delamination interface between $[0]$ and $[90]$ plies were fabricated using resin film infusion (RFI) technique. The thickness of each ply was 0.33 mm. In each laminate, there were three plies (two $[0]$ plies and one $[90]$ ply); so, the thickness of each laminate was 0.99 mm. The fabrication technique for $[0/90/0]$ laminate with a 40 mm delamination length, with delamination interface between $[0]$ and $[90]$ plies has been described below.

Four GFRP cross-ply laminates each of 0.99 mm thickness with $[0/90/0]$ lay-up were prepared using RFI technique. A resin film was sandwiched between the two plies. Such sandwiches were placed one above the other till the desired thickness was reached. A brass strip of 0.05 mm thick, 40 mm width (delamination length), and 100 mm length (80 mm length was kept inside the laminate and remaining 20 mm was projecting out) was inserted between 90° and 0° plies from one of the sides of the laminate. The brass strip was coated with poly vinyl alcohol for easy removal from the

laminate after curing. Sufficient bleeder was used to absorb any excess resin. A vacuum bag was placed on the top and sealed with a sealant tape. A thermocouple was placed on the top of the job to continuously monitor the temperature during curing. The job was heated at a rate of $2^\circ\text{C}/\text{min}$ up to 80°C , soaked for 30 min followed by heating up to 120°C and soaked for 60 min. After completion of heating cycle, the job was allowed to cool to room temperature. The brass strip was removed by subjecting to four point bending. Thus, a delamination of 40 mm length was created in the laminate. The laminate was cut into length and width of 400 and 300 mm, respectively. The lamina properties of this laminate are given in Table 1.

The same fabrication technique (RFI) as described above was used for making laminate of $[0/90/0]$ lay-up with 35 mm delamination size. Delaminations introduced in two laminates of $[0/90/0]$ lay-up, divided each laminate into two sub-laminates, $[0/90]$ and $[0]$, at the delamination region.

Experimental setup

The schematic experimental setup, as shown in Figure 4, consists of a signal generator, power amplifier, 200-MHz A/D card, signal conditioner, and a laptop computer. The probes used were contact probes mounted on variable angle shoes, which were made with perspex material. Water was used as couplant between the interfaces, i.e. probe and angle shoe, laminate, and angle shoe. The central frequency of excitation was 0.5 MHz and there were five cycles. The angle of the transducer to be set, based on the phase velocity of Lamb mode (S_0) to be generated and received, was calculated using Snell–Descartes law. Phase velocity of S_0 mode in GFRP laminate was obtained from DISPERSE.

A-scans from experiments

The distance of separation between the transmitter and receiver was fixed at 120 mm (approximately). The angle of transducers with respect to vertical was adjusted at 44.26° . Initially, the transmitter and receiver were positioned at healthy region. There was no delamination in the propagation path of S_0 mode from the transmitter to receiver. The A-scan obtained at this region is shown in Figure 5(a). Now, the transmitter and receiver were moved in such a manner that the delamination of size 40 mm was in between them. Figure 5(b) shows A-scan obtained in this configuration. Similarly, one more A-scan was captured, which is shown in Figure 5(c), keeping the delamination of size 35 mm in between the transmitter and receiver.

On each experimental A-scan, video envelope was fitted, and the peak of this envelope was taken as the representative arrival time of that wave group. Table 3 lists the arrival times of S_0 wave groups in each delamination case. The group velocities of S_0 mode in the sub-laminates [0] and [0/90] obtained from DISPERSE were 4765.9 m/s and 2757.7 m/s, respectively. The sizes of delaminations, estimated using Equation (2) were shown in Table 3.

Results and discussion

Numerical simulations were carried out on cross-ply laminates introducing four delaminations of different sizes from 70 mm to 50 mm. Table 3 lists the arrival times and difference in arrival times of Lamb mode, S_0 . The difference in arrival time decreases with decrease in the size of delamination, as shown in Table 3. This can also be deduced from Equation (2), which gives an estimate of the size of delamination. In Equation (2), the size of interface delamination is directly proportional to the difference in the arrival times of S_0 modes.

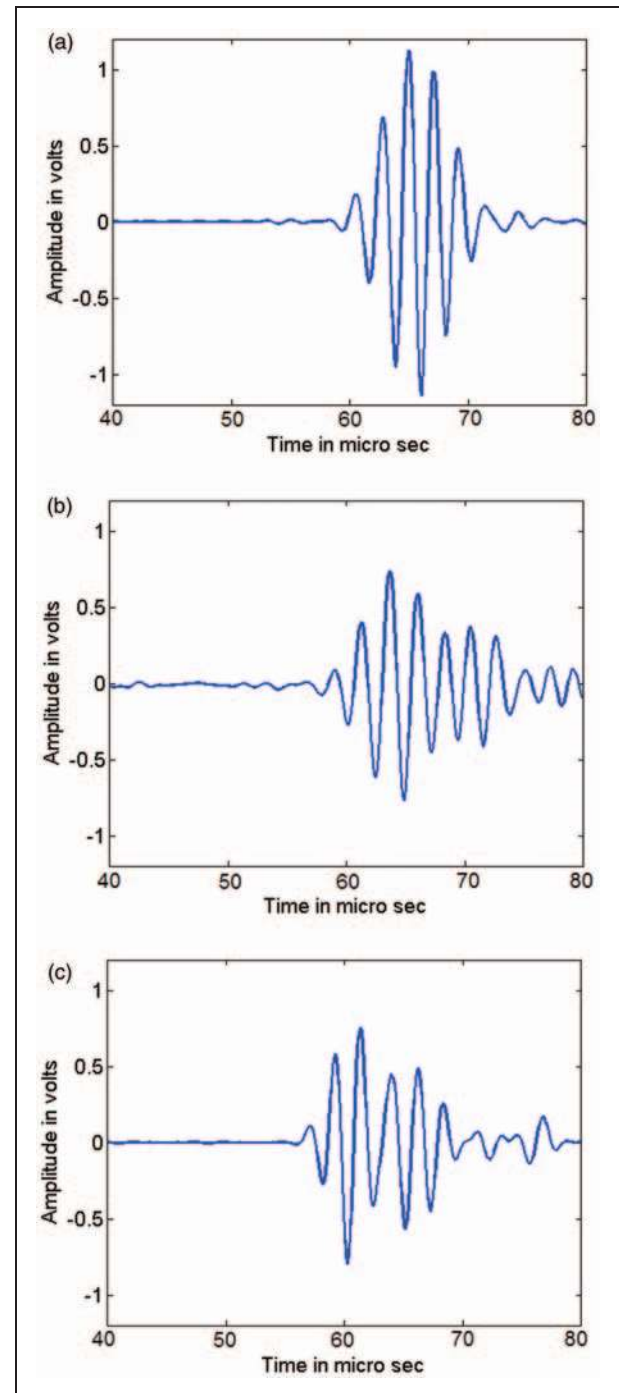


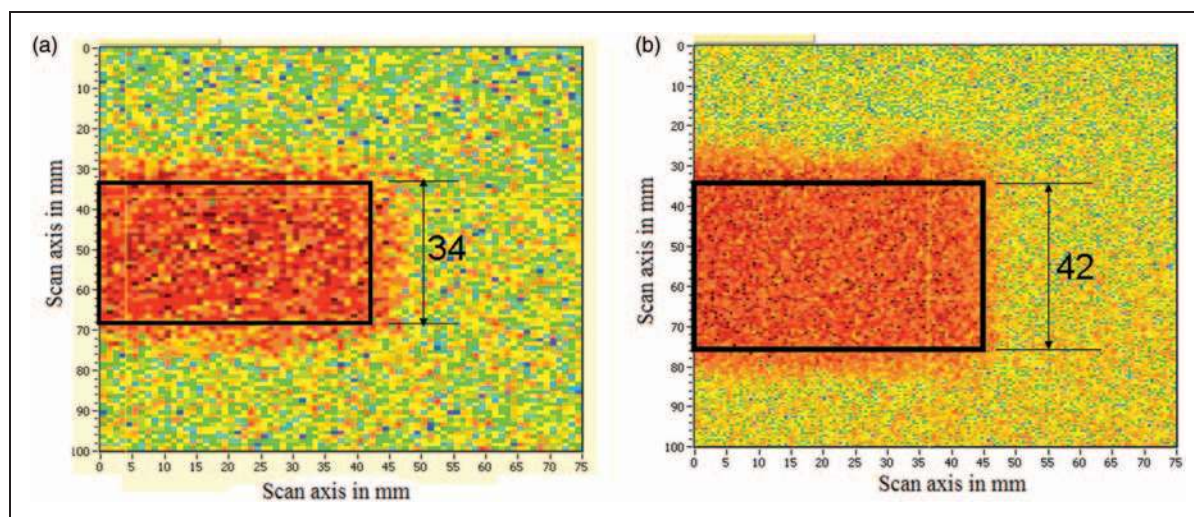
Figure 5. A-scans from experiments captured at (a) 0 mm, (b) 40 mm, and (c) 35 mm delamination locations.

The delamination sizes predicted using Equation (2) are in concord with the actual values.

Ramadas et al.²⁰ while proposing a methodology to predict the delamination size using A_0 and S_0 modes derived an expression to estimate the minimum size of detectable delamination (L_{\min}). This expression requires the group velocities of A_0 and S_0 mode

Table 3. Predicted delamination sizes from arrival times of S_0 modes in experiments on [0/90/0] laminate

Actual delamination size (mm)	t_1 (μs)	t_2 (μs)	$\Delta t = t_2 - t_1$ (μs)	Predicted delamination size, L (mm)
35	60.9	66.0	5.1	33.4
40	64.1	71.0	5.9	38.6

**Figure 6.** C-scan images obtained over (a) 35 mm and (b) 40 mm delamination regions.

velocities. In this study, S_0 modes were used for the prediction of delamination size. Based on this, the expression²⁰ can be modified as follows:

$$\frac{n}{2f} = L_{\min} \left(\frac{1}{V_1} - \frac{1}{V_2} \right) \quad (3)$$

where f and n are the excitation frequency and number of cycles, respectively. In numerical simulations, since, the excitation frequency (200 kHz), number of cycles (five) and the group velocities of S_0 mode were known, the estimated minimum size of detectable delamination (L_{\min}) was 45 mm. Figure 3(f) shows A-scan obtained through numerical simulations carried out on a cross-ply laminate containing 45 mm delamination. In this A-scan, since there is interference between S_0 modes propagating through the thin and thick sub-laminates, it is difficult to identify the arrival time of each S_0 mode. In such cases, to use this methodology, a suitable algorithm which can separate the signals undergoing interference, may have to be employed. Experimental validations were carried out on [0/90/0] cross-ply laminates containing 40 and 35 mm delamination sizes at the interface of 0° and 90° layers. The arrival times of S_0 modes in experimental A-scans were obtained by fitting a video envelope over the signal. Thus, obtained arrival times and difference in arrival times are listed in Table 3. Using the group velocities of S_0 mode in the

sub-laminates ([0] and [0/90]) and the difference in arrival times, the estimated delamination sizes were 38.6 and 33.4 mm, whereas the actual sizes were 40 and 35 mm, respectively. The predicted delamination sizes are in concurrence with the actual values. Conventional C-scan was carried out on delaminated regions. Figure 6 shows the C-scan images obtained over 35 and 40 mm delamination regions. The predicted sizes of delaminations from C-scan images were 34 and 42 mm. The minimum size of detectable delamination was also estimated in [0/90/0] laminate. This value worked out to 32 mm.

From the above discussion, it is concluded that in cross-ply laminates, ($[0/90]_{ns}$ and $[0/90]_{ms}$), the size of delamination at the bottom interface can be determined using the ToF of S_0 mode in 0° layer and the rest without any base line data or reference signal.

Conclusions

An expression, which can predict the size of delamination at the bottom interface without recourse to a reference signal, was derived. This expression was verified through numerical simulations and eventually validated by experiments. An existing expression for prediction of the minimum size of detectable delamination was modified to suit this study and used to predict the minimum size of detectable delamination in both numerical simulations and experiments.

Acknowledgments

The authors gratefully acknowledge the help rendered by Dr Rahul Harshe and Mr. Vinod Durai Swami, all from R & D E (E) for fabrication of laminates by RFI process.

Funding

This research received no specific grant from any funding agency in the public, commercial, or not-for-profit sectors.

References

- Rose JL. *Ultrasonic waves in solid media*. Cambridge, UK: Cambridge University Press, 1999.
- Guo N and Cawley P. The interaction of Lamb waves with delaminations in composite laminates. *J Acoust Soc Am* 1993; 94: 2240–2246.
- Guo N and Cawley P. Lamb wave reflection for the quick non-destructive evaluation of large composite laminates. *Mater Eval* 1994; 52: 404–411.
- Toyama N, Okabe T, Takeda N and Kishi T. Effect of transverse cracks on Lamb wave velocity in CFRP cross-ply laminates. *J Mater Sci Lett* 2002; 21: 271–273.
- Toyama N, Kikushima Y and Takatsubo J. Effect of delamination on Lamb wave velocity in cross-ply laminates. *J Mater Sci Lett* 2002; 21: 1891–1893.
- Dayal V and Kinra VK. Leaky Lamb waves in anisotropic plate. II: nondestructive evaluation of matrix cracks in fiber reinforced composites. *J Acoust Soc Am* 1991; 89: 1590–1598.
- Tang B and Henneke II EG. Lamb wave monitoring of axial stiffness reduction of laminated composite plates. *Mater Eval* 1989; 47: 928–934.
- Seale MD, Smith BT and Prosser WH. Lamb wave assessment of fatigue and thermal damage in composites. *J Acoust Soc Am* 1998; 103: 2416–2424.
- Valdes SHD and Soutis C. Real-time nondestructive evaluation of fiber composite laminates using low-frequency Lamb waves. *J Acoust Soc Am* 2002; 111: 2026–2033.
- Ho Ip K and Wing Mai Y. Delamination detection in smart composite beams using Lamb waves. *Smart Mater Struct* 2004; 13: 544–551.
- Su Z and Lin Y. Lamb wave based quantitative identification of delamination in CF/EP composite structures using artificial neural algorithm. *Compos Struct* 2004; 66: 627–637.
- Dufflo H, Morvan B and Izbicki JL. Interaction of Lamb waves on bonded composite plates with defects. *Compos Struct* 2007; 79: 229–233.
- Toyama N and Takatsubo J. Lamb wave method for quick inspection of impact-induced delamination in composite laminates. *Compos Sci Technol* 2004; 64: 1293–1300.
- Hayashi T and Kawashima K. Multiple reflections of Lamb waves at a delamination. *Ultrasonics* 2002; 40: 193–197.
- Liu GR and Achenbach JD. Strip element method for stress analysis of anisotropic linear elastic solids. *J Appl Mech* 1994; 61: 270–277.
- Liu GR, Xi ZC, Lam KY and Shang HM. A strip element method for analyzing wave scattering by a crack in an immersed composite laminate. *J Appl Mech* 1999; 66: 898.
- Palacz M, Krawczuk M and Ostachowicz W. The spectral finite element model for analysis of flexural-shear coupled wave propagation. Part: 2. Delaminated multilayer composite beam. *Compos Struct* 2005; 68: 45–51.
- Ramadas C, Balasubramaniam K, Joshi M and Krishnamurthy CV. Interaction of primary anti-symmetric Lamb mode with symmetric delaminations: numerical and experimental studies. *Smart Mater Struct* 2009; 18(8): 085011.
- Ramadas C, Balasubramaniam K, Joshi M and Krishnamurthy CV. Interaction of guided Lamb waves with an asymmetrically located delamination in a laminated composite plate. *Smart Mater Struct* 2009; 19(6): 065009.
- Ramadas C, Balasubramaniam K, Joshi M and Krishnamurthy CV. Delamination size detection using time of flight of anti-symmetric and mode converted A₀ mode of guided Lamb waves. *J Intell Mater Syst Struct* 2010; 21(6): 817–825.
- Choi HY, Downs RJ and Chang FK. A new approach toward understanding damage mechanisms and mechanics of laminated composites due to low-velocity impact: Part I – Experiments. *J Compos Mater* 1991; 25: 992–1011.
- Choi HY and Chang FK. A model for predicting damage in graphite/epoxy laminated composites resulting from low-velocity point impact. *J Compos Mater* 1992; 26: 2134–2169.
- Jih CJ and Sun CT. Prediction of delamination in composite laminates subjected to low velocity impact. *J Compos Mater* 1993; 27: 684–701.
- Li CF, Hu N, Yin YJ, Sekine H and Fukunaga H. Low-velocity impact-induced damage of continuous fiber-reinforced composite laminates. Part I. An FEM numerical model. *Composites Part A* 2002; 33: 1055–1062.
- Li CF, Hu N, Cheng JG, Fukunaga H and Sekine H. Low-velocity impact-induced damage of continuous fiber-reinforced composite laminates. Part II. Verification and numerical investigation. *Composites Part A* 2002; 33: 1063–1072.
- Sridharan S (ed.). *Delamination behavior of composites*. Cambridge, UK: Woodhead Publishing Ltd, CRC Press.
- User's manual Release 11*. Canonsburg, PA: ANSYS Inc, 2007.
- Lowe MJS. Disperse version 2.0.16b, Imperial College, London, UK, 2003.